Metallurgy

Tuba Yener*, Saadet Guler, Azmi Erdoğan, Kadir Mert Doleker, Suayb Cagri Yener and Alperen Refik Bilal Ozsarı

Kinetic study on nickel aluminides formed on Monel 400 alloy

https://doi.org/10.1515/mt-2025-0017
Published online April 14, 2025

Abstract: In this study on low temperature aluminized Monel 400 alloy, the growth kinetics of the aluminide layer are reported. Ni-based super alloy samples were aluminized for 2, 4, and 6 h at 600, 650, 700, and 750 °C, respectively. The morphologies and types of aluminides that developed on the Monel 400 substrate surface were examined using energy dispersive X-ray spectroscopy (EDS), scanning electron microscopy (SEM), and X-ray diffraction analysis (XRD). The thickness of the boride layer varied between 4 and 40 μm. The temperature and duration time of treatment had an impact on the hardness of the aluminides that developed on the samples, ranging from 800 to 250 HV. By altering the treatment's temperature and duration, the reaction's kinetics were also determined. A regression model was utilized to create an equation that can estimate the thickness of the aluminized layer based on the parameters of time and temperature. The projected values of the thickness of the aluminized layers were compared to the corresponding measurements obtained through experimentation, and a satisfactory agreement was achieved. Furthermore, a contour diagram is a recommended tool for determining the appropriate thicknesses of aluminized layers based on the prospective industrial applications of Monel 400.

Keywords: aluminizing; halide-activated pack cementation (HAPC); Monel 400; kinetics

1 Introduction

Candidate alloys for use in the chemical and maritime industries that require effective protection against corrosion and oxidation at high temperatures are nickel-based alloys [1], [2], such as Monel [3], [4]. Specifically, it is well known that Monel 400 exhibits exceptional resistance to corrosion in environments like saltwater, seawater, and strong acids (such HF and H_3PO_4). Nevertheless, Monel 400 is not appropriate for industrial applications involving heavy wear (erosion, cavitation, abrasive wear, and abrasive wear) due to its intrinsically low hardness such as 250 HV [5]. Extreme service conditions cause wear and corrosion in machines and equipment, which results in significant financial losses. These materials must have better surface properties in order to reduce such losses. In many papers, it was noted that these alloys' weak oxidation resistance at low temperatures roughly 500 °C limits their application. Coatings are a solution that have been well studied and are one of the options considered to address this issue [6]–[11]. One of the most popular methods for obtaining protective coatings to parts that must function at high temperatures is halide-activated pack cementation, (HAPC). The commonly used chloride salts for pack cementation process are NH_4Cl, NaCl, and $AlCl_3$, which are the salts considered here. For an efficient pack cementation process, the amount of halide activator added is normally controlled in the range of 1–5 wt.% [12]. Thus, the method is easy to apply, affordable, and useful. Pack cementation is the process of creating a gaseous transfer medium, which carries the active species to the substrate's surface [2], [13]. The metallic coating agent is carried to the substrate by gaseous halides formed by the heating of the chemical activator. This results from a partial pressure gradient between the low-thermodynamic-activity substrate and the

***Corresponding author: Tuba Yener**, Department of Metallurgy and Materials Engineering, Faculty of Engineering, Sakarya University, 54050, Sakarya, Türkiye, E-mail: tcerezci@sakarya.edu.tr
Saadet Guler, Faculty of Engineering and Architecture, Department of Metallurgical and Materials Engineering, University of Izmir Katip Celebi, 35620, Izmir, Türkiye
Azmi Erdoğan, Department of Mechanical Engineering, Faculty of Engineering, Bartın University, Bartın, Türkiye
Kadir Mert Doleker, Department of Metallurgical and Materials Engineering, Ondokuz Mayis Universitesi, 55139, Samsun, Türkiye
Suayb Cagri Yener, Department of Electrical and Electronics Engineering, Sakarya University, 54050, Sakarya, Türkiye; and Sakarya University Center for Electromagnetic Applications and Researches (SEMAM), Sakarya University, 54050, Sakarya, Türkiye
Alperen Refik Bilal Ozsarı, Institute of Natural Sciences, Sakarya University, 54050, Sakarya, Türkiye; and Türkiye Technology Team Foundation, Teknofest, Uşak province, Türkiye

high-thermodynamic-activity powder mixture. Dissociation of halides at the substrate surface results in the deposition of metal, which produces a composition gradient that promotes solid-state diffusion to the substrate [2], [13]–[15].

The mechanisms underlying the creation of aluminide coatings and the variables that affect their stability are still unclear, in contrast to the boride, nitriding coating formation mechanisms, which have been thoroughly investigated.

This work consequently attempted to investigate the mechanisms responsible for the development of aluminide diffusion coatings on a specific Ni based alloy, Monel 400, plates with a special focus on their high-temperature production kinetics of the coatings and their composition. Our research is the first to investigate how the thickness of the aluminized layer varies with temperature and time for Monel 400 alloy and to perform regression analysis and statistical examination in this context, as described in the literature review above.

2 Experimental

Monel 400 alloy was used as a substrate material in this study. Ni-based Cu-Ni alloy is a grade with a composition range of 28–34 max. Cu, 2.5 Fe, 0.3 C, 2 Mn, 0.5 Si, 0.024 S, balance Ni. The samples were placed in a cylindrical crucible filled with pack powder after being ground between 60 and 1,200 grit on SiC papers and cleaned with alcohol. A single specimen was placed inside the crucible, and every experiment's specimen location was precisely the same thanks to careful planning and execution. In order to consolidate the pack powder, it was filled all the way to the top of the crucible. The crucible was then sealed from the outside using a high temperature cement and coated with an alumina lid. A schematic representation is seen in Figure 1.

The coating procedure was applied at a temperature between 600 and 750 °C in an open atmosphere furnace. All the specimens were furnace-cooled after being exposed to the coating temperature for a predetermined amount of time, and the heating rate utilized was 10 °C min^{-1}. The microstructures of the coated specimens were examined using (SEM, Model JEOL JSM-6060, Japan) with an energy dispersive spectroscopy (EDS) performed to determine the distribution of alloying elements and equipped with energy dispersive spectroscopy (EDS). Rigaku X-ray diffractometer (DMAX 2200) with a Cu Kα radiation source of a wavelength of 1.541 Å over a range from 20° to 80° was used to analyze the phases generated on the surface layer of both bare and treated specimens. The microhardness values of the specimens were determined by a Vickers diamond pyramid indenter using a load of 25 g and dwell time 10 s.

3 Results and discussion

3.1 SEM-EDS and XRD analyses

Using an abrasive cutting tool, the sections of the aluminized samples were cut from the mid-section to reveal their cross sections as shown in Figure 2 from SEM-EDS analyses. It is seen that the coating layer increases due to increasing process temperature. In addition, oxidation is visible in the upper part of the coating layer, and it is clear that oxygen does not enter the interior part of the sample. In the experiment performed at 700° processing temperature, it was found that an aluminum oxide layer formed on the surface, despite the fact that the coating thickness increased with increasing temperature. It's evident that the coating starts to erode significantly as the process temperature reached to 750°.

The formation of the nickel–aluminum intermetallic phase during the pack cementation process can be viewed in two ways [16]: either the formed alloy phase reacts with the active aluminum or nickel atoms to form other types of alloy phases, or Al on the substrate surface or diffusing into the interior of the coating reacts with nickel atoms to form a nickel–aluminum phase. Looking at the SEM-Map Anayses

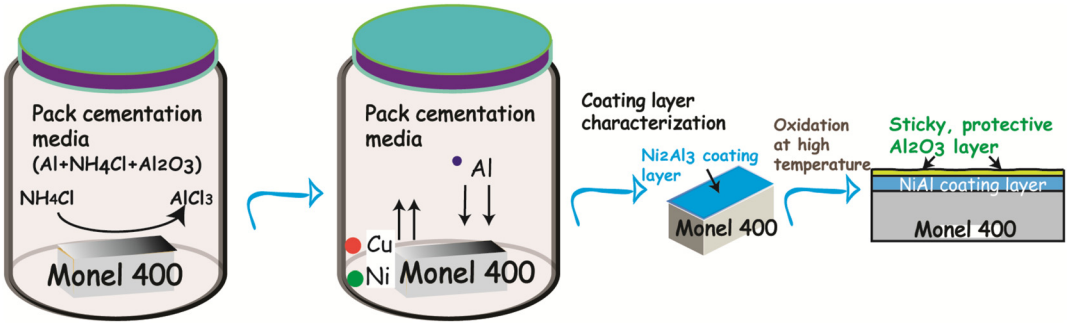

Figure 1: Schematic representation of pack aluminizing process.

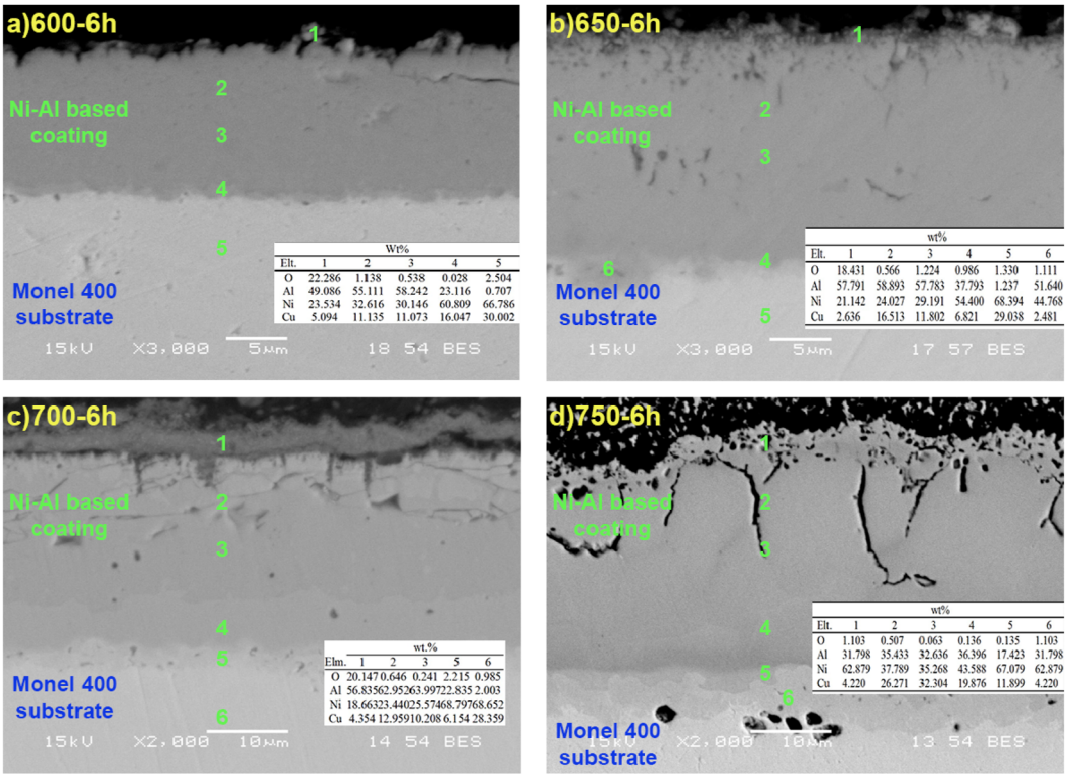

Figure 2: SEM and EDS analyses of aluminized Monel 400 samples for 6h; a) 600°C, b) 650°C, c) 700°C.

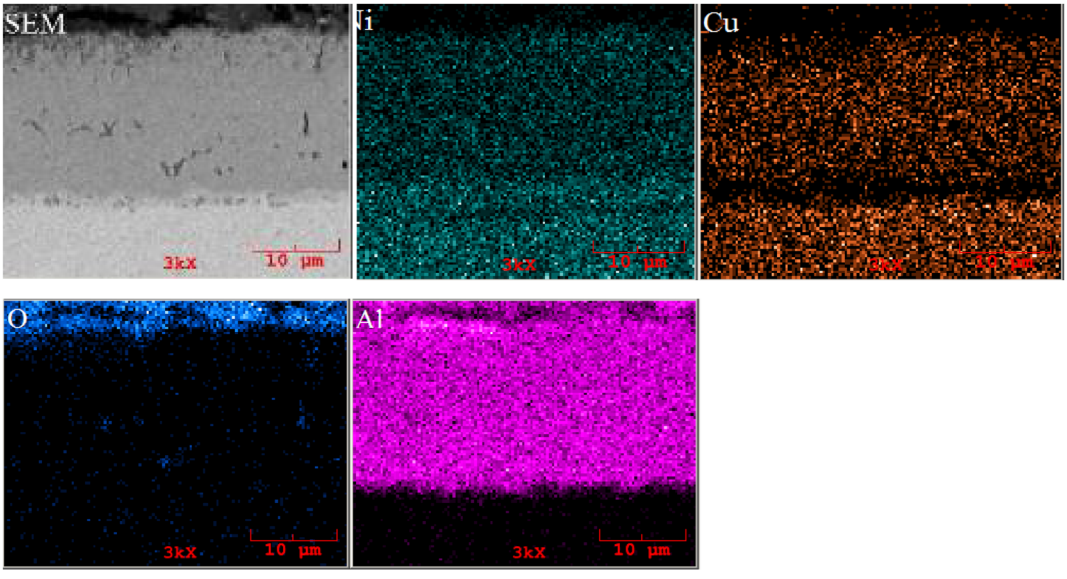

Figure 3: SEM and EDS analyses of 650 °C–6 h aluminized Monel 400 alloy.

Figure 3, Al deposition on the surface is seen clearly, and it is evident Ni and Cu elements are also transported densely to the coating layer. A thin layer appears as the kirkendal voids at the interface of the coating and the matrix. This thin zone can be clearly seen in SEM-map analyses.

Cu and Ni elements were both transported in the vicinity of the substrate in the Monel 400 alloy, resulting in an intermetallic that is Ni-rich Ni_3Al. Ni_2Al_3 is also main phase on the coating. XRD analyses also support EDS analyses Figure 4.

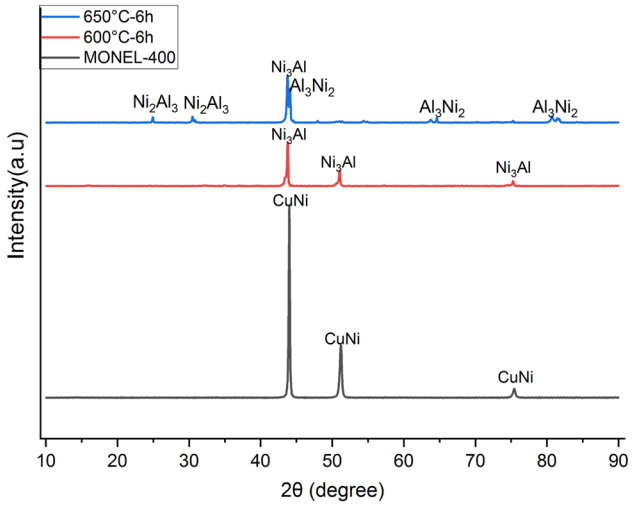

Figure 4: Xrd analyses of aluminized Monel 400 alloy with different temperatures.

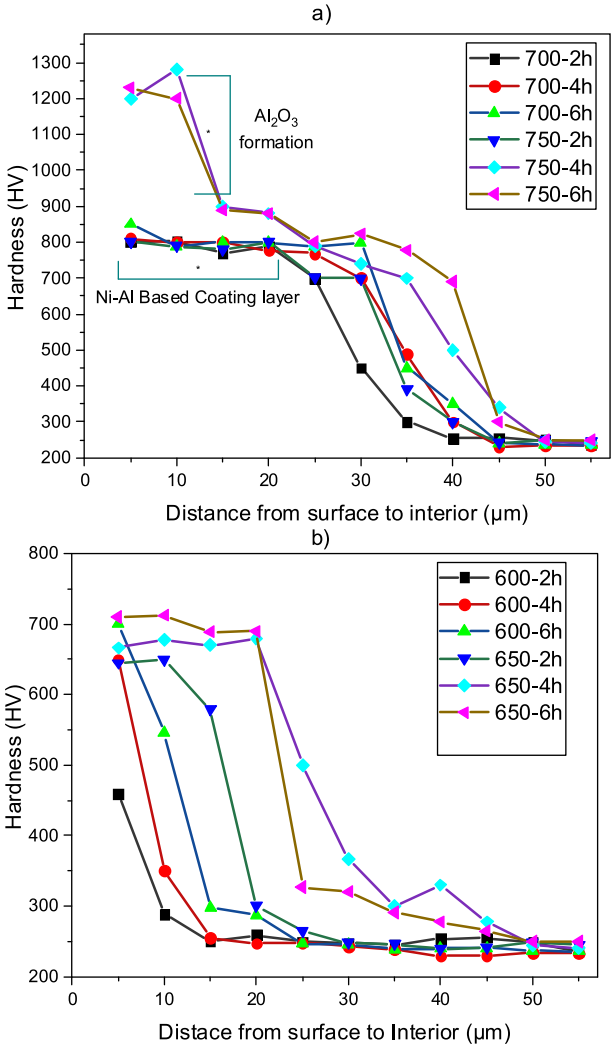

Figure 5: Hardness values at different times and at different distances from aluminized interiors of the Monel 400 alloy: a)700-750°C, b)600-650°C.

3.2 Hardness

A Vickers pyramid indenter with a 25 g applied stress and a 15 s dwell time was applied, which was used to assess the microhardness along the cross sections of the produced layers from surface to interior. The hardness value for each depth was calculated as the average of five measurements. While the matrix hardness was approximately 250 HV, the intermetallic phases that developed in the coating enhanced its hardness (Figure 5). Increasing the coating's temperature and duration also led to a more intense accumulation and hardness increase. Al_2O_3 was generated on the surface of the coatings produced at high temperatures of 700–750 °C. The hard ceramic phase also enhanced the hardness of the coatings, resulting in a hardness of around 1250 HV, or nearly five times that of the matrix.

3.3 Kinetics

It is necessary to understand certain kinetic parameters, including temperature and time, to regulate the aluminizing procedure. This study investigated how the temperature and aluminizing time affected the aluminide layer's development kinetics ("Equation (1)"). Diffusion coefficient values were primarily computed using "Equation (2)" or assuming unidirectional diffusion and parabolic growth of aluminum, the following equation can be used to describe the change in aluminide layer thickness over time:

$$d^2 = D \cdot t \tag{1}$$

with D: growth rate constant ($cm^2\ s^{-1}$), t: process time (s), and d: depth of the aluminide layer (cm).

The relationship between the activation energy, Q, temperature, and growth rate constant, D, may be said to be able to be written as an Arrhenius equation [17]–[19].

$$D = D_0 \cdot \exp - (Q/RT) \tag{2}$$

with Q is the activation energy (kJ $mole^{-1}$), D is the diffusion coefficient ($cm^2\ s^{-1}$), T is the absolute temperature (K), and R is the gas constant ($J\ mol^{-1}\ K^{-1}$). The layer thickness is displayed for the time intervals of 2, 4, and 6 h. Diffusion constant values for 600 °C–750 °C have been determined by taking into account experimental layer thickness values.

The natural logarithm of the rate constant versus the reciprocal inverse of the aluminizing temperature in $Kelvin^{-1}$ shows a linear connection in accordance with "Equation (2)" and the slope in that equation yielded the activation energy of 117 kJ mol^{-1} for the Monel 400 alloy. By tracking the depth of the aluminide layer as a function

of process temperature and time, the growth kinetics of the layer are examined (Figure 6).

Günen et al. [3] studied pack-boriding process of Monel 400 alloy in the temperature range of 1,173–1,273 K for exposure times of 2–6 h. The boron activation energy in the Ni_2B layer was estimated as equal to 300.7 kJ mol^{-1} in their study. Yener et al. [18] studied aluminizing effect on a Fe-Cr-Ni super alloy and for a range of 550–500 °C; 2, 4, 6 h, the activation energy value was 207 kJ mol^{-1}

3.4 Prediction of aluminite layer thickness by a regression model

The thickness of the aluminite layer in the coating process is contingent upon the temperature and time of the procedure. According to the experimental results, the contour diagram showing the coating thickness depending on time and temperature is given in Figure 7. A full factorial model with 2 factors at 3 levels was employed to forecast the thickness of the aluminite layer with respect to time and temperature [20]. By employing this methodology, "Equation (3)" has been obtained.

$$d = -123.4 + 2.125t + 0.204T \quad (3)$$

with t: aluminizing time (h) and T: temperature (°C).

The aluminized time (h) is represented by t, and T represents the temperature in degrees Celsius. "Equation (3)" can be utilized to generate the contour diagram illustrated in Figure 7.

Table 1 shows a comparison between the measured thicknesses of aluminized layers and the values predicted by "Equation (3)" within the temperature range of 600–750 °C. A reasonable correlation was found between the experimental and simulated data sets, with an average standard deviation of around ±1.72 µm. Yalamaç et al. [21]. obtained a similar situation in their study on boriding kinetics. The experimental data and the data generated through regression were comparable. Upon examination of this diagram, it is possible to determine the thickness of the aluminized layer at different temperatures and times. These diagrams can serve as a reference in industrial applications.

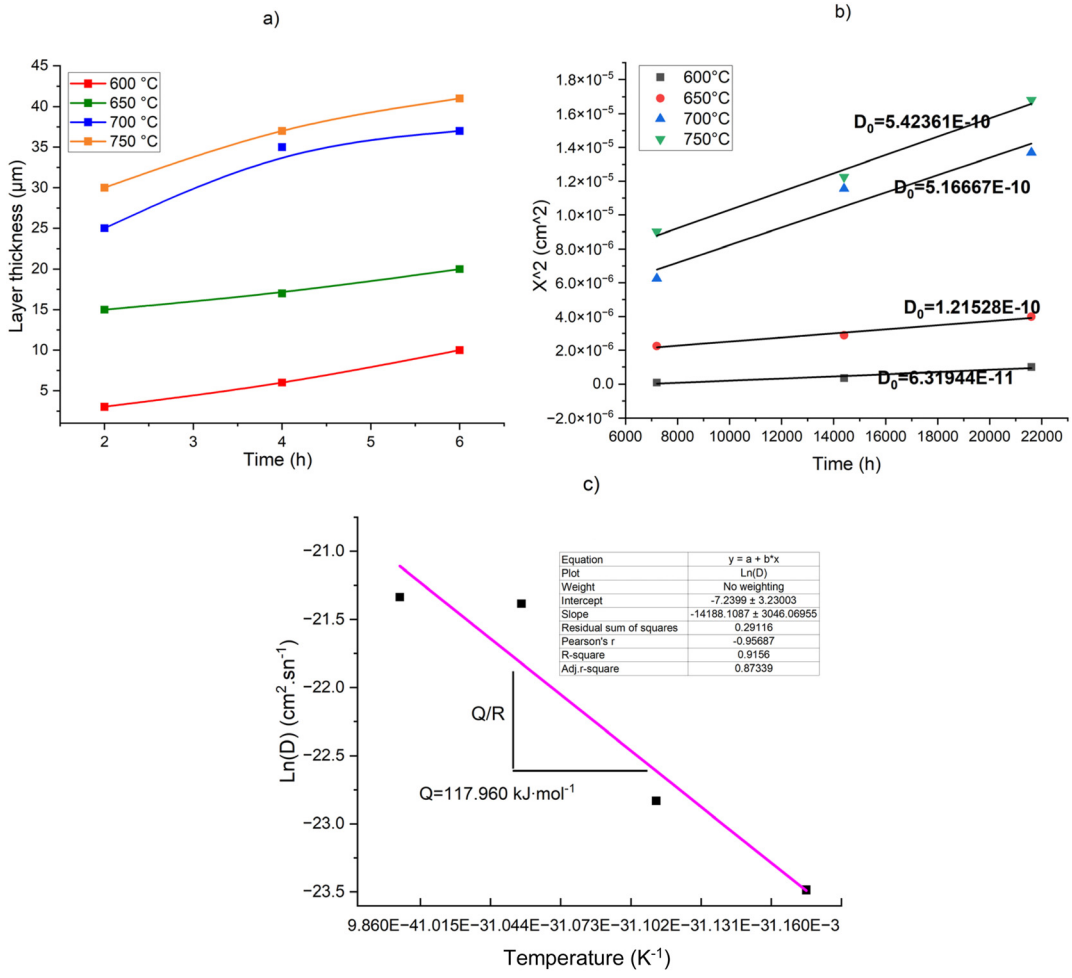

Figure 6: Growth kinetics of aluminide layer on Monel 400, a) layer thickness, b) square of aluminide layer thickness versus time, and c) the growth rate constant according to the Arrhenius equation.

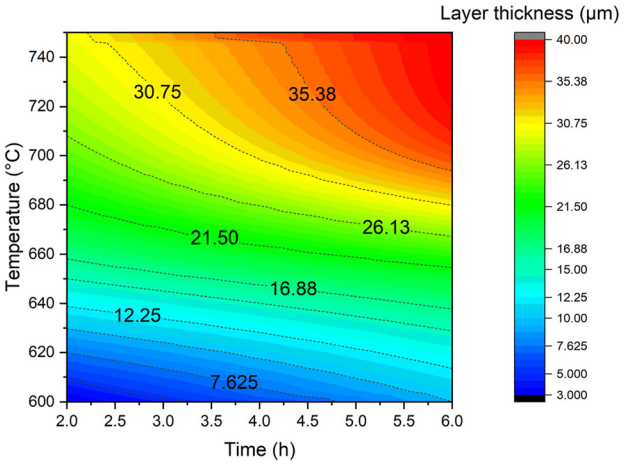

Figure 7: Contour diagram describing the evolution of the aluminized layer thickness as a function of the aluminized parameters.

Table 1: Measured values of the thickness of the aluminum layer values predicted by the regression model (simul.).

Temperature (°C)	Time (h)	Layer thickness, (μm)	
		Exp.	Simul.
600	2	3	3.25
	4	6	7.5
	6	10	11.75
650	2	15	13.75
	4	17	17.7
	6	20	21.95
700	2	25	23.65
	4	35	27.9
	6	37	32.15
750	2	30	33.85
	4	36	38.1
	6	40	42.35

Table 1 presents a comparison was conducted between the measured values of the thickness of the aluminum layer at temperatures ranging from 600 °C to 750 °C and the values predicted by the regression model (simul.).

In summary, based on experimental results, layer thickness appears to be an important temperature and time dependent factor. To demonstrate the impact of the aluminum layer on temperature and time, statistical analysis was conducted using Nested ANOVA (Analysis of Variance). The ANOVA test findings in Table 2 clearly demonstrate that both temperature and time have a substantial impact on the thickness of the aluminized layer. Upon analysis of the data, it was found that the F-statistic is 25.734 and the p-value is 0.0002, indicating that temperature has a significant effect ($p < 0.05$) on the total aluminized layer thickness. Temperature affects the variation in coating thickness more than time.

Table 2: Analysis of variance (ANOVA) test results for aluminized layer thickness.

Source	DF	SS	MS	*F*	*P*
Temperature (°C)	3	1,647.00	549.00	25.734	0.0002
Time (h)	8	170.66	21.33		
Total	11	1,814.66			

Table 3: Variance components results for aluminized layer thickness.

Source	Var comp.	% of total
Temperature (°C)	175.88	89.10
Time (h)	21.33	10.82
Total	197.22	

Table 3 presents an ANOVA analysis that illustrates the distribution of total variance across different factors. The thickness of the aluminized layer is mainly affected by temperature, with time having a minor impact.

4 Conclusions

(1) The aluminide layers formed on super alloy is compact, porosity free, and good adhesion.
(2) The presence of Ni_2Al_3, Ni_3Al phases in the aluminide layers were confirmed by XRD. The hardness of aluminide phase according to treatment time and temperature are changing between 250 and 900 HV, which can be determined from hardness diagrams.
(3) The growth rate constants and activation energies of the aluminide layers in the process conditions were in good agreement with study and detected as 117 kJ mol^{-1}. Practical formulas derived from classical kinetics equations were to give good layer thicknesses results, which are too closely to experimental data.
(4) The experiment yielded an equation using regression analysis conducted using the Minitab software. The coefficient of determination (R^2 value) for the resulting equation is 93.81. The layer thicknesses obtained through experimentation and the data derived from the regression equation exhibited strong agreement. Highly similar values were acquired.
(5) Furthermore, a contour diagram was constructed to illustrate the relationship between temperature, time, and the thickness of the aluminized layer. Through the examination of this diagram, one can make predictions about the thickness of the aluminized layer at various temperatures and durations.

Acknowledgments: The authors would like to express their thanks to Metallurgy and Materials Engineer, Baybora Kılıç, Onur Can Ateş, Ferziye Kartboga, Nergis Kıral for their positive support during experimental studies.

Research ethics: Not applicable.

Informed consent: Not applicable.

Author contributions: The authors have accepted responsibility for the entire content of this manuscript and approved its submission.

Use of Large Language Models, AI and Machine Learning Tools: None declared.

Conflict of interest: The authors state no conflict of interest.

Research funding: None declared.

Data availability: The raw data can be obtained on request from the corresponding author.

References

[1] T. Yener, *et al*., "Wear and oxidation performances of low temperature aluminized IN600," *Surf. Coat. Technol.*, vol. 436, 2022, Art. no. 128295, https://doi.org/10.1016/j.surfcoat.2022.128295.

[2] Ş. H. Atapek, C. K. Gencay, T. Yener, F. Kahrlman, and G. A. Çelik, "Effect of pack characteristics and process parameters on the properties of aluminide-coated Inconel 625 alloy," *Mater. Test.*, vol. 65, no. 11, pp. 1657–1667, 2023, https://doi.org/10.1515/MT-2023-0125/MACHINEREADABLECITATION/RIS.

[3] A. Günen, M. Keddam, A. Erdoğan, and M. Serdar, "Pack – boriding of Monel 400 : microstructural characterization and boriding kinetics," *Met. Mater. Int.*, vol. 28, no. 8, pp. 1851–1863, 2022, https://doi.org/10.1007/s12540-021-01066-8.

[4] S. C. Yener, A. R. B. Özsarı, K. Doleker, A. Erdogan, and T. Yener, "Microstructure and oxidation of a Ni–Al based intermetallic coating formation on a Monel-400 alloy," *Mater. Test.*, vol. 66, no. 8, pp. 1138–1144, 2024, https://doi.org/10.1515/mt-2024-0038.

[5] Y. Küçük, K. M. Döleker, M. S. Gök, S. Dal, Y. Altınay, and A. Erdoğan, "Microstructure, hardness and high temperature wear characteristics of boronized Monel 400," *Surf. Coat. Technol.*, vol. 436, 2022, Art. no. 128277, https://doi.org/10.1016/J.SURFCOAT.2022.128277.

[6] M. Sabri, A. Erdo, M. Öge, A. Günen, and E. Kanca, Dry sliding wear behavior of borided hot-work tool steel at elevated temperatures," *Surf. Coat. Technol.*, vol. 328, pp. 54–62, 2017, https://doi.org/10.1016/j.surfcoat.2017.08.008.

[7] T. Teker and M. Sarl, "Metallurgical properties of boride layers formed in pack boronized cementation steel," *Mater. Test.*, vol. 64, no. 9, pp. 1332–1339, 2022, https://doi.org/10.1515/MT-2022-0098/MACHINEREADABLECITATION/RIS.

[8] Y. Li, F. Xie, and X. Wu, "Microstructure and high temperature oxidation resistance of Si–Y co-deposition coatings prepared on TiAl alloy by pack cementation process," *Trans. Nonferrous Met. Soc. China*, vol. 25, no. 3, pp. 803–810, 2015, https://doi.org/10.1016/S1003-6326(15)63666-4.

[9] Y. B. Zhou, H. Chen, H. Zhang, and Y. Wang, "Preparation and oxidation of an Y2O3-dispersed chromizing coating by pack cementation at 800 °C," *Vacuum*, vol. 82, no. 8, pp. 748–753, 2008, https://doi.org/10.1016/J.VACUUM.2007.10.010.

[10] F. Aydin, A. Ayday, M. E. Turan, and H. Zengin, "Role of graphene additive on wear and electrochemical corrosion behaviour of plasma electrolytic oxidation (PEO) coatings on Mg–MWCNT nanocomposite," *Surf. Eng.*, vol. 36, no. 8, pp. 791–799, 2020, https://doi.org/10.1080/02670844.2019.1689640.

[11] Ç. Demirbaş and A. Ayday, "Effect of Ag concentration on structure and wear behaviour of coatings formed by micro-arc oxidation on Ti6Al4 V Alloy," *Surf. Eng.*, vol. 37, no. 1, pp. 24–31, 2021, https://doi.org/10.1080/02670844.2020.1741211.

[12] X. J. Lu and Z. D. Xiang, "Formation of chromium nitride coatings on carbon steels by pack cementation process," *Surf. Coat. Technol.*, vol. 309, pp. 994–1000, 2017, https://doi.org/10.1016/J.SURFCOAT.2016.10.047.

[13] B. A. Pinto, A. Sofia, and C. M. Oliveira, "Surface & Coatings Technology Nb silicide coatings processed by double pack cementation : formation mechanisms and stability," *Surf. Coat. Technol.*, vol. 409, 2021, Art. no. 126913, https://doi.org/10.1016/j.surfcoat.2021.126913.

[14] T. Yener, A. Erdogan, M. S. Gök, and S. Zeytin, "Formation, characterization, and wear behavior of aluminide coating on mirrax® ESR steel by low-temperature aluminizing process," *J. Tribol.*, vol. 143, no. 1, pp. 1–8, 2021, https://doi.org/10.1115/1.4047667.

[15] A. Erdogan, T. Yener, K. M. Doleker, M. E. Korkmaz, and M. S. Gök, "Low-temperature aluminizing influence on degradation of nimonic 80A surface: microstructure, wear and high temperature oxidation behaviors," *Surf. Interfaces*, vol. 25, 2021, https://doi.org/10.1016/j.surfin.2021.101240.

[16] T. Yener, K. Mert, A. Erdogan, M. Oge, and Y. Er, "Surface & Coatings Technology Wear and oxidation performances of low temperature aluminized IN600," *Surf. Coat. Technol.*, vol. 436, 2022, Art. no. 128295, https://doi.org/10.1016/j.surfcoat.2022.128295.

[17] S. Sen, U. Sen, and C. Bindal, "The growth kinetics of borides formed on boronized AISI 4140 steel," *Vacuum*, vol. 77, no. 2, pp. 195–202, 2005, https://doi.org/10.1016/j.vacuum.2004.09.005.

[18] T. Yener, "Low temperature aluminising of Fe-Cr-Ni super alloy by pack cementation," *Vacuum*, vol. 162, pp. 114–120, 2019, https://doi.org/10.1016/j.vacuum.2019.01.040.

[19] I. Uslu, H. Comert, M. Ipek, F. G. Celebi, O. Ozdemir, and C. Bindal, "A comparison of borides formed on AISI 1040 and AISI P20 steels," *Mater. Des.*, vol. 28, no. 6, pp. 1819–1826, 2007, https://doi.org/10.1016/j.matdes.2006.04.019.

[20] C. De Recherche, N. De Draria, A. Brahimi, and A. Sehisseh, "Diffusion kinetics of boron in the X200CrMoV12," *J. Min. Metall., Sect. B*, vol. 51, no. 1, pp. 49–54, 2015, https://doi.org/10.2298/JMMB140404009A.

[21] E. Yalamac, İ. Türkmen, and Ö. Fırtına, "Characterization and kinetic analysis of iron boride layer formed on the GGG 70 ductile cast iron," *Trans. Indian Inst. Met.*, vol. 74, no. 7, pp. 1701–1711, 2021. https://doi.org/10.1007/s12666-021-02249-y.

The authors of this contribution

Tuba Yener

Dr. Tuba Yener graduated from Sakarya University, Department of Metallurgical and Materials Engineering, Turkey. She received her MSc and PhD degrees from Sakarya University, Department of Metallurgical and Materials Engineering. She is currently working as Assoc. Prof. Dr. at Sakarya University, Faculty of Engineering, Metallurgy and Materials Engineering. Her interests are in the intermetallic materials, materials characterization, and surface properties of materials.

Saadet Guler
Dr. Saadet Guler graduated from Sakarya University, Department of Metallurgical and Materials Engineering, Turkey. He received his MSc degree from Dokuz Eylul University, Phd Degree from Dokuz Eylul University Department of Metallurgical and Materials Engineering. He is currently working as an expert at İzmir Katip Celebi University, Faculty of Engineering, Metallurgy and Materials Engineering. His interests are on polymeric materials, materials characterization, and high entropy alloys.

Azmi Erdoğan
Dr. Azmi Erdoğan graduated from Bartin University, Department of Metallurgical and Materials Engineering, Turkey. He received his MSc and PhD degrees from Sakarya University, Department of Metallurgical and Materials Engineering. He is currently working as Assoc. Prof. Dr. at Bartin University, Faculty of Engineering, Materials Division. His interests are in the metallic materials, materials characterization, and wear.

Kadir Mert Doleker
Dr Kadir Mert Doleker graduated from Sakarya University, Department of Metallurgical and Materials Engineering, Turkey. He received his MSc degree from Sakarya University, Department of Metallurgical and Materials Engineering. He is currently working as an Assoc. Prof. Dr. at 19 Mayis University, Faculty of Engineering, Metallurgy and Materials Engineering. His interests are on oxidation properties of materials, materials characterization, and surface properties of materials.

Suayb Cagri Yener
Dr. Suayb Cagri Yener graduated from Sakarya University, Department of Electric and Electronic Engineering, Turkey. He received his MSc and PhD degrees from Istanbul Technical University, Department of Electric and Electronic Engineering. He is currently working as Assoc. Prof. Dr. at Sakarya University, Faculty of Engineering, Electric Division. His interests are electromagnetic fields, memristors, and mathematical modeling.